



Unveiling the Nature of Polar-ring Galaxies from Deep Imaging

Aleksandr V. Mosenkov^{1,2} , Vladimir P. Reshetnikov^{2,3}, Maria N. Skryabina³, and Zacory Shakespear¹ 

¹ Department of Physics and Astronomy, N283 ESC, Brigham Young University, Provo, UT 84602, USA; aleksandr_mosenkov@byu.edu

² Central (Pulkovo) Astronomical Observatory, Russian Academy of Sciences, Pulkovskoye Chaussee 65/1, 196140 St. Petersburg, Russia

³ St. Petersburg State University, 7/9 Universitetskaya Nab., 199034 St. Petersburg, Russia

Received 2022 July 27; revised 2022 August 23; accepted 2022 August 25; published 2022 October 12

Abstract

General structural properties and low surface brightness tidal features hold important clues to the formation of galaxies. In this paper, we study a sample of polar-ring galaxies (PRGs) based on optical imaging from the Sloan Digital Sky Survey Stripe 82 and other deep surveys. We investigate the deepest images of candidates for PRGs to date. We carry out photometric decomposition on the host galaxies and associated polar structures that allows us to derive the structural properties of both components. We are able to detect very faint tidal structures around most PRGs in our sample. For several galaxies, we can directly observe the formation of the polar ring due to merging, which is manifested in debris of the victim galaxy and an arc-like polar structure made up of its material. In a few cases, we can discern signs of tidal accretion. The results obtained indicate that the gravitational interaction and merging of galaxies are the most plausible mechanisms for the formation of PRGs.

Key words: methods: data analysis – techniques: photometric – galaxies: structure

1. Introduction

Polar-ring galaxies (PRGs) are among the most beautiful and unusual objects in the universe. We are used to the fact that galaxies are flat, held by regular rotation, or almost spherical, supported by random motions of stars. However, there are objects that do not fit into this simple scheme. They embody a strange symbiosis—an early-type galaxy and a spiral one in the same object. Numerous examples of such objects are given in Whitmore et al. (1990) (=PRC, Polar Ring Catalogue), Moiseev et al. (2011) (=SPRC, SDSS-based Polar Ring Catalogue) and Reshetnikov & Mosenkov (2019) (new candidates for PRGs).

The main characteristic feature of PRGs is that they contain two large-scale, morphologically and kinematically decoupled subsystems—the central galaxy (the host) and the polar structure (PS). (In this paper we will use the term “PRG” to designate the whole class of galaxies with near-polar optical structures, without dividing into polar-disk or PRGs—e.g., Iodice 2014.) These two subsystems of PRGs exhibit very different characteristics. In most cases their central objects look like early-type galaxies without gas, with relatively red color indices and rotation around their minor axes (e.g., Whitmore et al. 1987; Finkelman et al. 2012; Reshetnikov & Combes 2015). On the other hand, PSs (in most cases their major axes are almost orthogonal to the major axes of the central galaxies) contain stars and gas, which rotate around the major axes of the central galaxies. They have blue colors and show signs of ongoing star formation; the gas in such structures often has sub-solar metallicity (e.g., Whitmore et al. 1987;

van Gorkom et al. 1987; Reshetnikov & Combes 1994, 2015; Egorov & Moiseev 2019). The unique morphology of PRGs makes them very useful laboratories for studying a number of extragalactic astronomy issues linked to the formation and evolution of galaxies, and for exploring the properties of their dark haloes (see Combes et al. 2014; Khoperskov et al. 2014 and references therein).

To explain the observed structure of PRGs, a number of, at times considered exotic, formation mechanisms were proposed. For instance, Sérsic (1967b) suggested that the PS of NGC 4650A is a string of clouds of relativistic electrons ejected from the nucleus of the galaxy. For NGC 2685—the first known PRG (Burbidge & Burbidge 1959)—it has been suggested that the central object in the galaxy represents the result of an explosion in a preexisting spiral galaxy outlined by the rings (Gorbatskii & Korovyakovskii 1979). The structure of UGC 7576 has been interpreted as an edge-on spiral galaxy with a prominent bulge aligned orthogonally to the disk (Mould et al. 1982).

The most popular explanation for the structure of PRGs originates from Alar Toomre’s comment that in the case of NGC 2685 we may be seeing the accretion of an intergalactic gas cloud or “a small, gas-rich companion in the not too distant past” (Toomre 1977). In the same year, a similar idea was expressed in the work of Knapp et al. (1977). A few years later, Shane (1980) discussed external accretion to explain the structure of NGC 2685 in more detail. Schweizer et al. (1983) expanded the accretion scenario and included the possibility of “the accretion of material transferred between two galaxies during a close encounter”.

Currently, there are several scenarios for the formation of PRGs due to interaction of galaxies with their environment, such as:

–Major merger: a head-on collision of two galaxies with their disks oriented perpendicularly (Bekki 1997, 1998; Bournaud & Combes 2003). This scenario is particularly able to explain the presence of two ring structures in ESO 474-G26 as a transient stage in the merging of two spiral galaxies (Reshetnikov et al. 2005). Also, the delayed return of tidally ejected material during the merging can lead to the formation of PSs (Hibbard & Mihos 1995).

–Minor merger: a tidal disruption of a small companion in a near-polar orbit of the host galaxy. This mechanism could only explain narrow unclosed rings (e.g., Johnston et al. 2001; Reshetnikov et al. 2006).

–Tidal accretion: a gas-rich donor galaxy loses matter to form the ring around the host (Reshetnikov & Sotnikova 1997; Bournaud & Combes 2003). The donor galaxy must be on a nearly polar orbit with respect to the host galaxy. An example of applying this scenario to a giant spiral galaxy AM 1934-563 is presented in Reshetnikov et al. (2006). In addition, several interacting systems are observed in which matter is directly transferred from one member to another with the formation of a large-scale PS (e.g., NGC 3808A/B, NGC 6285/86 – Reshetnikov et al. 1996; Ordenes-Briceño et al. 2016).

–Infall of gas from intergalactic space: a cold accretion of gas along cosmological filaments (Thakar & Ryden 1996, 1998; Maccio et al. 2006; Brook et al. 2008). A candidate for a PRG formed in this way is described by Stanonik et al. (2009).

As such, half of these scenarios are related to galaxy mergers which underpin our current understanding of how galaxies grow and evolve under the Λ CDM paradigm. However, it is likely that, depending on the spatial environment and properties of the galaxies themselves, different mechanisms for the formation of PRGs can be realized. To understand how a particular object formed, we have to acquire detailed photometric and spectral observations, as well as carry out a study of its environment.

A very important window for looking into the past of any galaxy is its study at very low levels of surface brightness. Ultra-deep images of galaxies can reveal the “scaffolding” preserved from the time of their formation – tidal tails and bridges, stellar haloes, envelopes, plumes, etc. If the formation of PRGs is associated with accretion of matter, we can expect to detect traces of these processes at the periphery of galaxies. Unfortunately, deep images of PRGs are very rare. For instance, Finkelman et al. (2010) presented a deep image of a candidate to PRGs in the Subaru Deep Field. They described several extended low surface brightness (LSB) features around the galaxy which can indicate an ongoing merging with a companion. Finkelman et al. (2012) discussed the morphology of 16 PRG candidates based on the original photometry and the Sloan Digital Sky Survey (SDSS) Stripe 82 data (Jiang et al. 2008). They noted, in

particular, signs of recent interactions in several galaxies (asymmetric tails, stellar fans, etc.).

In this pilot study, we exploit ultra deep images of 13 PRG candidates from the SDSS Stripe 82 and other modern deep optical surveys in order to shed more light on the possible origin of the PSs. We focus on revealing LSB structures in and around PRGs and pay special attention to the quantitative and qualitative description of these features. Temporal fine structures, such as tidal tails, streams and shells with survival times ~ 1 Gyr (see e.g., Mancillas et al. 2019; Rampazzo et al. 2020, and references therein), should be good indicators of the forming PRG structures. This allows us to carry out a detailed photometric analysis of the deep images of PRGs. We also perform photometric decomposition for the entire sample and study the properties of the host and PS.

This paper is outlined as follows. We present our sample in Section 2. Section 3 gives a description of the data and image preparation. In Section 4, we present in detail the properties for each of the selected galaxies. We discuss our results in Section 5. Our findings are summarized in Section 6. Throughout this article, we adopt a standard flat Λ CDM cosmology with $\Omega_m = 0.3$, $\Omega_\Lambda = 0.7$, $H_0 = 70 \text{ km s}^{-1} \text{ Mpc}^{-1}$. All magnitudes and colors in the paper are given in the AB-system and corrected for the Milky Way extinction (Schlafly & Finkbeiner 2011) and k -correction (Chilingarian et al. 2010).

2. The Sample

Our sample is composed of 13 objects from the SPRC (Moiseev et al. 2011) located in the field of Stripe 82. The list of galaxies, along with their general characteristics taken from the SDSS DR15 (Aguado et al. 2019), is presented in Table 1. The galaxies in the table are divided into four groups in accordance with the SPRC original classification: three galaxies are classified as the best candidates for PRGs, five are good candidates, four objects are galaxies possibly related to PRGs and one object is classified as a possible face-on ring. As can be seen from Table 1, the sample galaxies are bright objects with $g - r$ color typical of PRGs (e.g., Reshetnikov & Mosenkov 2019).

Our visual inspection of the SDSS frames reveals that most of the sample galaxies indeed demonstrate pronounced PSs (see Section 3). In eight cases, the PSs look symmetric (SPRC-1, 4, 69, 73, 77, 185, 188, 234), and in three they show a large-scale asymmetry (SPRC-74, 76, 238). The visible orientation of two galaxies (SPRC-186 and 275) and our photometric decomposition (see Section 4) do not allow us to conclude that they have polar features. Section 4 provides a detailed description of each object from our sample. In Table 1, we briefly summarize our notes on each object.

3. Data and Preparation

For our study, all images of the selected galaxies are taken from the SDSS Stripe 82 Imaging Data reduced by Jiang et al. (2014).

Table 1
Basic Properties of the Sample Galaxies

SPRC type	Galaxy	R.A. (J2000)	Decl. (J2000)	z (1)	M_r (mag) (2)	$g - r$ (3)	Faint features (4)
Best candidates	SPRC-1	00:09:12	-00:36:55	0.07325	-22.01	0.80	Diffuse light, tidal tails and streams, faint polar halo
	SPRC-4	02:42:58	-00:57:09	0.04299	-19.43	0.57	Tidal streams
	SPRC-69	20:48:06	+00:04:08	0.02467	-19.66	0.88	...
Good candidates	SPRC-73	00:32:10	+01:08:37	0.05909	-21.31	0.76	Curved tidal tail
	SPRC-74	00:48:12	-00:12:56	0.05646	-21.12	0.73	Curved tidal tail, arc, plume, bridge
	SPRC-76	01:21:29	+00:37:29	0.04356	-19.56	0.77	Curved tidal tail, plume, bridge
	SPRC-77	01:58:58	-00:29:23	0.08112	-20.41	0.81	Oval polar envelope, bridge?
	SPRC-185	23:12:32	-00:06:37	0.02783	-20.45	0.74	Boxy polar envelope, plume, bridge?
Related objects	SPRC-186	00:48:10	-00:54:44	0.03397	-21.17	0.76	...
	SPRC-188	03:34:06	+01:05:40	0.04748	-21.21	0.81	Tidal streams, plume
	SPRC-234	21:23:39	-00:22:35	0.06198	-20.51	0.79	Very faint grand-design spiral structure or (un?)closed polar ring or projection?
	SPRC-238	23:39:58	+00:08:07	0.06018	-21.70	0.62	Straight tidal tail, arc, bridge?
Possible face-on ring	SPRC-275	20:53:53	-00:58:05	0.10610	-21.01	0.82	...

Note. (1) redshift; (2), (3) absolute magnitude in the r band and $g - r$ color respectively; (4) see Section 4 where we describe each galaxy in detail.

To prepare galaxy images, we employ a semi-automatic image preparation pipeline `IMage ANalysis`⁴ (IMAN, see Mosenkov et al. 2020). It is important to note that standard SDSS frames have a depth of $26.5 \text{ mag arcsec}^{-2}$ in the r band, whereas the average depth of the images, downloaded from the Stripe 82 database in the same band, is $28.89 \pm 0.25 \text{ mag arcsec}^{-2}$. Here and below we compute the photometric depth as a 3σ fluctuation in square boxes of $10'' \times 10''$. The small standard deviation of the photometric depth for our sample shows that the presence of low-contrast structures in the images under study should be detected nearly in the same way for all galaxies. Below, we briefly describe our methodology for preparing stacked cut-outs of the sample galaxies (see Mosenkov et al. 2020 for detail). To exploit the Stripe 82 data to their fullest, that is to increase the depth of these observations and unveil very faint structures around the galaxies, we stack the Stripe 82 images in the three gri -bands (the u and z bands are shallow as compared to the gri bands, Fukugita et al. 1996), similar to what was done by Miskolczi et al. (2011) and Morales et al. (2018) but for standard SDSS data.

First, we employ `SExtractor` (Bertin & Arnouts 1996) to create a segmentation map for each image. In this map, the size of every object is increased by a factor of 1.5 to reduce the scattered light from the detected sources when subtracting the sky background. Then, we iteratively approximate the sky using polynomials, starting with 1st order. If necessary, we increase the polynomial order for a less flat sky background. Fortunately,

all images do not show a significant non-flat background or Galactic cirri (only SPRC-1 and SPRC-188 have adjacent filamentary clouds with $\langle \mu_r \rangle \sim 26.8 \text{ mag arcsec}^{-2}$ in the r band which do not directly overlap the galaxies). We also examined the Schlegel et al. (1998) reddening map and found moderate $E(B - V) = 0.05 \pm 0.03$ for the coordinates of the sample galaxies. Therefore, we can be confident that neither the subtraction of the sky, nor dusty filaments in our Galaxy affect the LSB regions around the sample galaxies.

We carry out the above described procedures for all three gri bands of the Stripe 82 data and resample the prepared images in the g and i bands to the r band using the `pypher`⁵ package (Boucaud et al. 2016). The Point-Spread Function (PSF) images for this resampling are taken from the IAC Stripe 82 Legacy Project database (Fliri & Trujillo 2016). To create an extended PSF for each image, we merge this downloaded image and use it as a core PSF (seeing), with the wings (beyond 9 pixels from the PSF center) of a unified extended PSF from Infante-Sainz et al. (2020). Finally, we stack the prepared galaxy images in the gri bands by applying the `IRAF/IMCOMBINE` procedure.

Applying `SExtractor` to each of the stacked images, we select good unsaturated stars with the highest signal-to-noise ratio. After that, we perform photometric calibration using the measured fluxes of these stars and their corresponding total magnitudes in the r band from the SDSS database. By doing so,

⁴ https://bitbucket.org/mosenkov/iman_new/src/master/

⁵ <https://github.com/aboucaud/pypher>

we are able to estimate the depth of the stacked images in the r band. It appears to be 29.74 ± 0.13 mag arcsec $^{-2}$ for the whole sample, almost one magnitude deeper than in the original deep r -band frames.

Finally, we mask out all sources, which do not belong to the target galaxies, using `SExtractor` and the `mtolibrary`⁶ (Teeninga et al. 2015). The latter package allows us to accurately mask foreground objects inside the galaxy’s outermost isophotes where `SExtractor` usually faces issues with creating a correct segmentation map.

We also prepare enhanced grz images (see Appendix) from the DESI Legacy Imaging Surveys DR8 (hereafter DESI Legacy, Dey et al. 2019), to ensure that the very faint features around the galaxies in the Stripe 82 images are also seen in other, independently obtained images (see Figure A1).

4. The Detailed Description of the Sample PRGs

In this section, we provide a brief description of each galaxy, with useful information on its structural properties based on our visual inspection of the final stacked images (see Figures 1 and A1) and the results of our multicomponent photometric decomposition which we present below. To our best knowledge, most galaxies in our sample have little or no information in the literature. The unprecedented depth of the stacked Stripe 82 images for these galaxies helps us explore very faint features around the selected PRGs in much more detail than previously done. We also compare the Stripe 82 and Legacy images, in order to confirm the presence of the same LSB features in both surveys. For several galaxies, Subaru Hyper Suprime-Cam (Aihara et al. 2022) observations are available, so we use them as well.

Throughout the paper, we refer to several types of LSB structures, some of which we define here in the following way (see e.g., Duc et al. 2015; Mancillas et al. 2019; Rampazzo et al. 2020). Tidal tails are elongated stellar structures which are generated by galaxy interactions and mergers (usually, major mergers). They are generally accepted as evidence for a dynamically cold (and/or often gas-rich disk) component in the accreted companion (Combes et al. 1995). Tidal tails are expelled from the primary galaxy following an interaction with a less massive companion. Thus, the material in the tail and the stellar halo of the primary galaxy should have similar properties, such as the same color. Recently, Ren et al. (2020) classified long tidal tails into three shape types: straight, curved and plume (in a form without a certain figure). They inferred that these shapes are associated with different formation mechanisms of tidal tails, e.g., with prograde (curved tails) and retrograde merging (plume tails).

In contrast, tidal streams are related to minor merging events when a low-mass satellite is interacting with a major galaxy

and, finally, can be ingested by it. The material of the tidal stellar stream is expelled from the accreted companion and, thus, should have essentially the same color as the satellite. Also, tidal streams look like long and thin filaments, usually fainter and thinner than tidal tails (Sola et al. 2022). However, according to hydrodynamical cosmological simulations in Mancillas et al. (2019), the lifetime of streams is, on average, longer (1.5–3 Gyr) than that of tidal tails, which become visible at a timescale of 0.7–1 Gyr after the start of the merger.

Also, we use the term “halo”, or “envelope” to describe the stellar outskirts of galaxies. This component is mainly a mixture of ancient halo stars formed in situ (Font et al. 2011; McCarthy et al. 2012; Cooper et al. 2015) and accreted stars due to a series of minor merger episodes in the past (Cooper et al. 2010, 2013). In this paper, we classify outer structures as envelopes if they are remarkably extended and diffuse (see good examples of galaxies with diffuse envelopes in Rich et al. 2019 and Mosenkov et al. 2020). Among other LSB features which we can notice around and in galaxies are strong asymmetric and disturbed outer structures, arcs, shells, fans and bridges.

Recently, Sola et al. (2022) measured the properties (the area, size and average surface brightness) for more than 8000 tidal structures around 352 nearby massive galaxies using deep images from the 3.6-meter Canada–France–Hawaii Telescope with approximately the same surface brightness limit as in the SDSS Stripe 82. One of the important conclusions of their study is that they do not detect any tidal features fainter than 27.5 mag arcsec $^{-2}$ in the r band. Therefore, in this study we expect to reveal all such LSB structures around PRGs, if they exist, and describe their properties.

For three PRGs in our sample (SPRC-73, 76 and 238), we quantitatively describe the tidal structures well-seen in the deep images. Here, by Ψ we denote the angle between the major axes of the host and the ring. To estimate some general luminance and geometrical parameters of the stellar structures in these galaxies, we outline them in the stacked images within an isophote of 27 mag arcsec $^{-2}$ (we apply blurring with $\sigma = 1$ pixel to reduce pixel to pixel variations). We define the average projected width W_{tail} and projected length of the tidal structure L_{tail} along the centerline, which connects the beginning and the end of the outlined region. Also, we compute an average surface brightness within the structure and its fraction to the total galaxy luminosity within the same isophote 27.5 mag arcsec $^{-2}$. We roughly estimate the color $g - r$ of the host, ring and tidal feature within the regions where these structures dominate. The results of our analysis are listed in Table 2 and shown in Figure A3 in the Appendix. As can be seen, the length of the tails of SPRC-73 and SPRC-238 is significantly longer and the width of the tail of SPRC-73 is ~ 4 times larger than typically found around ETGs (see Figures 9 and 10 in Sola et al. 2022), whereas their average surface brightness is of the same order as measured in the stellar tails and streams.

⁶ <https://github.com/CarolineHaigh/mtobjects>

Table 2
Properties of the Tidal Tails for the Three Polar-ring Galaxies Measured using the SDSS r -band Images

Galaxy	Ψ (deg)	L_{tail} (arcsec)	L_{tail} (kpc)	W_{tail} (arcsec)	W_{tail} (kpc)	$\langle \mu_{r,\text{tail}} \rangle$ (mag arcsec $^{-2}$)	f_{tail}	$(g-r)_{\text{tail}}$ (mag)	$(g-r)_{\text{h}}$ (mag)	$(g-r)_{\text{ps}}$ (mag)
(1)	(2)	(3)	(4)	(5)	(6)	(7)	(8)	(9)	(10)	(11)
SPRC-73	63	63.7	72.8	32.3	36.6	26.5 ± 0.3	0.032	0.61 ± 0.22	0.82	0.64
SPRC-76	86	29.0	24.9	11.7	10.0	25.6 ± 0.7	0.089	0.41 ± 0.12	0.99	0.48
SPRC-238	82	37.1	43.1	9.2	10.7	26.3 ± 0.3	0.018	0.69 ± 0.20	0.60	0.38

Note. We adopt the original classification from the SPRC. (1) Galaxy name; (2) angle between the major axes of the polar ring and host; (3), (4) projected length of the centerline of the tail; (5), (6) average projected width of the tail; (7) average surface brightness within the tail; (8) tail-to-total luminosity (within the isophote 27 mag arcsec $^{-2}$) ratio; (9), (10), (11) - colors of the tail, host and polar ring, respectively.

Finally, we carry out photometric decomposition for the entire sample in the r band. As we show below, using the results of decomposition we can i) analyze the parameters of the PS and the host, ii) reject non-PRGs and iii) seek the link of these parameters with the origin of the PRGs. Following Reshetnikov & Combes (2015), we use a Sérsic function (Sérsic 1967a, 1968) to describe both the host and PS. The free parameters of the Sérsic function are the surface brightness μ_e at the effective (half-light) radius r_e , the Sérsic index n (which controls the shape of the luminosity profile), the position angle PA, the ellipticity ϵ , and the C_0 parameter, which controls the disk/boxy view of the isophote (when $C_0 < 0$ the isophotes are disk, whereas they look boxy if $C_0 > 0$ and $C_0 = 0$ if the isophotes are pure ellipses). The decomposition is done by means of the IMFIT code (Erwin 2015) with the full treatment of the extended PSF.

In case when a tidal structure is present, we mask it in our fitting. SPRC-74 and 238 show arc-like features; SPRC-234 demonstrates two faint spiral arm-like structures. Therefore, for these galaxies we mask out these structures in our modeling which implies the presence of a rather symmetric polar component. For SPRC-1 and 275, the overlapping galaxies are fitted as well to better model the light distribution of the target galaxy. The results of the decomposition for the entire sample are listed in Table 3. In Figure A4 we present our 2D photometric models.

SPRC-1: This is a red early-type galaxy with a polar dust ring which is aligned almost orthogonally to the major axis of the host galaxy ($\Psi = 84^\circ.5$). Its optical spectrum is typical for active galactic nucleus galaxies with broad emission lines. Its polar dust structure looks like a nearly edge-on dust ring. The visible dust lane noticeably distorts the observed galaxy profile in the central region, therefore we mask it in our modeling. The optical diameter of the ring reaches 18 kpc (Reshetnikov et al. 2011). SPRC-1 is a member of a compact group of galaxies: it is surrounded by a handful of galaxies which demonstrate apparent tidal features. The outer profile of SPRC-1 is contaminated by the light of the other group members. Therefore, the multiple faint tidal features in the deep image are less apparent than in the other deep images of our sample galaxies. Two spiral galaxies near SPRC-1 show prominent grand-design structures (SDSS J000909.89-003705.3 has a

strong two-armed spiral, with one arm drawn to its smaller companion, the spiral galaxy SDSS J000911.73-003721.8), which might be induced by multiple tidal interactions within this group (see a review by Dobbs & Baba 2014). Interestingly, based on their spectra, most large members of this group demonstrate an activity typical for star-forming or starburst galaxies. Our decomposition reveals that apart from the polar dust ring, this galaxy also harbors a very luminous polar ($\Psi = 82^\circ.6$) halo (the PS-to-host ratio $L_{\text{ps}}/L_{\text{h}} = 0.98$) with the Sérsic index $n = 1.7$. This halo may have the same origin as the dust ring since both have very similar position angles. As galaxy interactions and merging are very intensive in compact groups, we can suppose that the formation of the PSs in this S0 galaxy can be related to a wet merger: a head-on collision between two orthogonally oriented galaxies, in which large quantities of gas and dust from another galaxy in this group could produce the polar dust disk and stellar halo we now observe.

SPRC-4: It is a kinematically-confirmed PRG (Moiseev et al. 2014). The deep image of this galaxy reveals the presence of a blue polar-ring which was previously noted by Finkelman et al. (2012). The small Sérsic index of the PS model $n = 0.2$ confirms that this structure is a ring. We notice two chain-like structures around SPRC-4 which seem to be spiraling toward the host galaxy. In fact, these structures can be parts of fainter extended loops of gaseous and stellar material. Finkelman et al. (2012) note at least 10 galaxies in the neighborhood of SPRC-4, some with the signatures of ongoing star formation. A close spiral galaxy to SPRC-4, SDSS J024256.42-005658.4, has, in fact, a different redshift (0.181) and thus cannot be gravitationally bound to SPRC-4. The nearest blue dwarf galaxy (its morphological type is not clear due to poor resolution), SDSS J024252.07-005646.6, is located at a projected distance of about 80 kpc and can be a potential donor of the gas for SPRC-4. We suggest that the ongoing star formation in the ring and its formation itself can be explained by the (tidal) accretion of gas or disruption of a gas-rich dwarf. In the case of tidal accretion, we suspect the blue dwarf galaxy SDSS J024252.07-005646.6 to be the donor (although its redshift is unknown).

SPRC-69 (II Zw 92): Its deep image displays that the outer, almost polar wide ring ($\Psi = 77^\circ.5$, $n = 0.3$) surrounds the central body ($n = 2.4$). The results of spectral observations

Table 3
The Results of Our Decomposition for the Stripe 82 Images in the r Passband

SPRC	m_h (mag)	$r_{e,h}$ (arcsec)	n_h	$(g-r)_h$	m_{ps} (mag)	$r_{e,ps}$ (arcsec)	n_{ps}	$(g-r)_{ps}$	Ψ (deg)	PS/Host
(1)	(2)	(3)	(4)	(5)	(6)	(7)	(8)	(9)	(10)	(11)
1	17.21	1.2	2.4	0.80	16.13	12.8	1.7	0.76	82.6	0.98
4	16.18	1.9	2.1	0.65	16.27	2.7	0.2	0.29	80.4	0.17
69	15.59	1.3	2.4	0.77	16.14	14.2	0.3	0.57	77.5	0.60
73	16.26	1.9	2.8	0.82	16.78	7.8	1.0	0.64	63.3	0.62
74	16.20	1.7	1.3	0.73	75 ⁺	...
76	17.38	1.4	6.1	0.99	17.82	4.2	0.7	0.48	86.0	0.67
77	17.93	1.27	17.53	2.9	0.1	0.47	89.2	0.39
185	15.84	0.74	17.58	4.1	1.5	0.66	70.6	0.20
186	16.09	1.3	1.0	0.51	15.34	3.6	0.6	0.82	27.1	2.00
188	15.57	6.7	1.0	1.01	17.21	10.0	0.5	0.22	83.2	0.22
234	16.75	2.1	1.8	0.72
238	15.59	3.3	1.5	0.54
275	18.41	1.1	1.5	0.86	17.68	6.7	0.2	0.31	18.9	1.45

Note. For SPRC-77, we only provide the total magnitude of the host since it is not resolved. In SPRC-185, the host is an S0 galaxy, which consists of a nucleus, a bulge and a disk, and, therefore, we only present the total magnitude for the superposition of these components. For SPRC-74, SPRC-234 and SPRC-238, the fitting was only carried out for the central galaxy. The total magnitudes and colors have been corrected for Galactic extinction and k -correction. (1) Galaxy name, (2) total r -band magnitude of the host, (3) effective radius of the host, (4) Sérsic index of the host, (5) $g-r$ color of the host, (6) total r -band magnitude of the PS, (7) effective radius of the PS, (8) Sérsic index of the PS, (9) $g-r$ color of the PS, (10) angle between the major axes of the PS and the host (for SPRC-74 it is estimated by hand) and (11) the PS-to-host luminosity ratio.

confirm the presence of a PS, in both ionized gas and stars (Moiseev et al. 2011). Along the major axis of the central body, Moiseev et al. (2011) also point out a linear increase in the rotation velocity of stars. Our deep and color images clearly show faint bound structures (spirals?) which start from the ends of the polar-ring. This may indicate that the polar ring is in fact a disk. There are two close dwarf galaxies (SDSS J204807.12+000416.3 and SDSS J204806.63+000332.8), but we cannot see any faint structural features related to these objects. Also, their spectroscopic redshifts are unknown. The regular structure of SPRC-69 down to very LSBs provides proof that this system is relatively old and relaxed. We suppose that the polar ring in this galaxy formed due to either a major merger (the contribution of the ring is substantial, $L_{ps}/L_h = 0.60$) or a tidal accretion followed by a merger with the donor after the formation of the ring (Reshetnikov & Sotnikova 1997; Bournaud & Combes 2003). The survival time for tidal tails and streams is up to $\approx 2-3$ Gyr (Mancillas et al. 2019; Rampazzo et al. 2020). Apparently, SPRC-69 should have started its formation earlier, so that we do not observe any fine structures around this galaxy in the current epoch.

SPRC-73: The spectrum of SPRC-73 is typical for star-forming galaxies. The major axis of the diffuse PS is inclined by $\Psi \sim 63^\circ$ with respect to the major axis of the host galaxy. There is also a bright blue point source (a bulge or a nucleus of the victim galaxy?) to the north of the center which lies exactly in the plane of the diffuse polar component and has the same redshift $z = 0.059$ as the host galaxy. In addition, we can see a faint arc with another red dwarf galaxy SDSS J003208.55+010834.5 to the west. Many small extended objects around

SPRC-73 may also be involved in the multiple (wet and dry) minor merging with the host galaxy (for example, there is a faint bridge with SDSS J003207.63+010847.4 at the northwestern outskirts of SPRC-73). This galaxy shows a giant curved tail in the deep image which bends around the host and extends about one arcmin (~ 70 kpc) to the south (see also Finkelman et al. 2012). The average surface brightness of the curved tail $\langle \mu_r \rangle \sim 26.6$ mag arcsec $^{-2}$ is beyond the depth of single-exposure SDSS frames, and, thus, it cannot be seen in them. We note that the colors of the polar ring and the tail are very similar and differ from the reddish color of the host. Thus, this tail is intimately related to the observed PS (its “current” profile is purely exponential $n = 1.0$). Therefore, we can conclude that the most plausible scenario to explain the forming PS in SPRC-73 is ongoing merging with a galaxy, the debris of which has not yet been dispersed. We find that the luminosity of the PS, including the tail and the nucleus, is rather high as compared to the host ($L_{ps+}/L_h = 0.75$). This is an indication of the major merger which leads to the formation of the PS in SPRC-73.

SPRC-74: A blue asymmetric elongated structure crosses the main body of SPRC-74 at an angle of about 75° to the major axis. The PS is strongly bent and displaced relative to the center of the host galaxy, which shows a Sérsic index close to exponential ($n = 1.3$). We can distinguish a diffuse, LSB galaxy of irregular shape on the northeastern side of SPRC-74 and a faint short stream to the east. The main body of the host galaxy demonstrates distorted outer isophotes and bends toward the diffuse LSB galaxy in the northeast. The disturbed shape of both the main and diffuse galaxies hints at the ongoing gravitational interaction. As noted in Finkelman et al. (2012), a

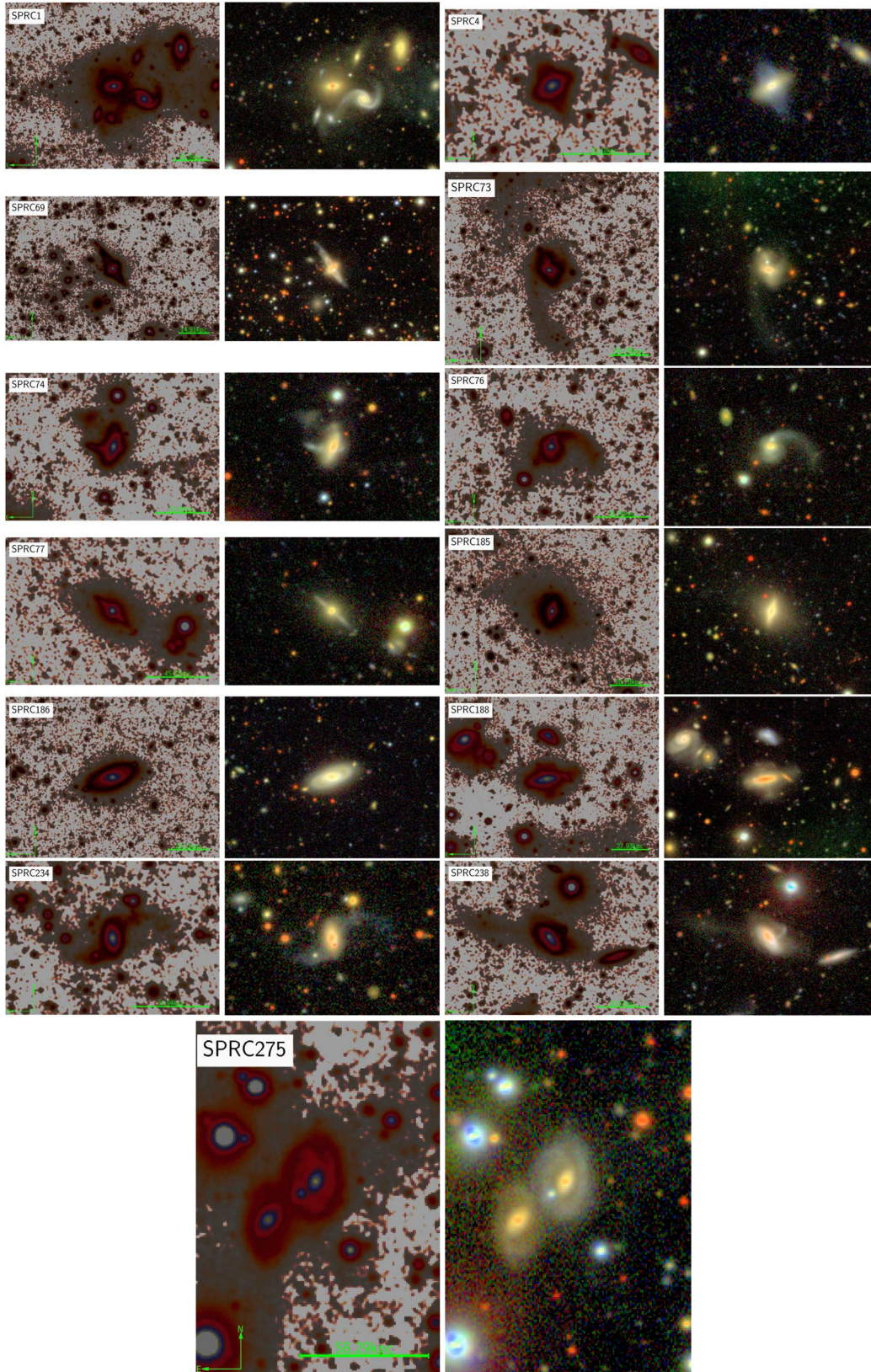


Figure 1. Stacked images (left panel) and color RGB images (right panel), created from the Stripe 82 images in the *g*, *r* and *i* bands. The stacked images have been blurred with $\sigma = 1$ pixel. Only pixels with surface brightnesses down to $28 \text{ mag arcsec}^{-2}$ are shown. The green bar depicts the scale $30''$.

close companion SDSS J004805.83-001251.2 lies at a projected distance of about $1'.6$ (~ 100 kpc) from SPRC-74. In our stacked image we can see an extended, thin stream directed to the west, which connects multiple clumpy objects (tidal dwarf galaxies?) up to $1'$ from the galaxy. Unfortunately, beyond that radius the scattered light from a close bright star pollutes our SDSS image. However, the Subaru Hyper Suprime-Cam image in Figure A2 shows much less scattered light from the bright star, so we can distinguish a faint ($\langle\mu_r\rangle \sim 26.6$ mag arcsec $^{-2}$) thin bridge connecting SPRC-74 and the closest blue spiral galaxy SDSS J004805.83-001251.2 ($z = 0.05661$). This fact leads us to suggest that the most probable scenario for this PRG is tidal accretion from the gas-rich neighbor.

SPRC-76: The red host galaxy in SPRC-76 is surrounded by the blue material of the merging galaxy, the debris (its profile has $n = 1.1$) of which we observe as the blue object SDSS J012129.26+003732.6 (it has a concordant $z = 0.04386$) with the blue curved tail emerging from it. Also, we can see a clear bridge (depicted by a maroon color in Figure 1) which connects the main body and the red satellite SDSS J012129.86+003719.7. Furthermore, we detect a plume on the eastern side of SPRC-76 to the north, up to another dwarf galaxy SDSS J012130.98+003745.6. Possibly, there is also a link with the spiral galaxy SDSS J012130.98+003745.6 to the northeast. We also detect a faint bridge with the LSB galaxy SDSS J012132.24+003758.6 which is located beyond the previously mentioned spiral in the same direction. The strongly distorted structure of SPRC-76 indicates that we observe a major merger which is likely to be responsible for the ongoing generation of the PS.

SPRC-77: Finkelman et al. (2012) note on SPRC-77 and 185 that they “resemble “normal” disk galaxies with a symmetric bright disk around their central bulge rather than typical PRGs”. However, careful examination of the deep image and its photometric decomposition reveals that SPRC-77 has a distinctive oval central component (the host), which is embedded in the blue wide polar ring ($n = 0.1$). This galaxy demonstrates quite regular inner and outer isophotes. Our deep image also reveals an oval envelope ($n = 1.1$), the major axis of which seems to be misaligned with the major axis of the ring.⁷ We can see a small southeastern arc in the plane of the disk which could be a dwarf satellite stretched by the tidal forces. The profiles of SPRC-77 and two southwestern interacting galaxies seem to have either a bridge or be overlapping, so there is not enough evidence to suggest that this system is gravitationally bound. Also, we observe several dwarf galaxies on the northeastern side of SPRC-77 which exhibit signatures (tidal streams and bridges) of interaction with the major galaxy.

⁷ We will consider this galaxy, along with SPRC-185, in a separate paper. Here we only present the results of our multicomponent (host+ring+halo) decomposition.

The regular shape of this envelope signifies that it has the same origin as the polar ring—a major merger in the past.

SPRC-185: SPRC-185 is another pure edge-on galaxy in our sample. The smooth outer structure, which is almost orthogonal to the central galaxy, becomes prominent only in our deep image. It has a boxy shape and does not resemble “normal” polar ring galaxies from our sample. Our decomposition model for this galaxy consists of a nucleus, a dominant bulge, a flared disk and a polar component with the Sérsic index $n \approx 1.5$. Thus, the PS in this galaxy is not a ring, but a halo. We also note a plume on the eastern side of the galaxy, which is probably related to the formation of the polar halo due to a merger.

SPRC-186: Our decomposition shows that this galaxy has a reddish inner disk (a pseudobulge with $n \approx 1$), a blue inner ring and two spiral arms (as a single component with $n = 0.6$), instead of an outer ring which might be interpreted as tilted with respect to the inner component. Therefore, this suggests that SPRC-186 is not a PRG. Unlike most PRGs in our sample, we see no LSB details around it.

SPRC-188: This highly inclined galaxy with a prominent dust lane shows a polar edge-on structure ($\Psi \sim 83^\circ$), which is slightly off the center and is more pronounced in the south direction than to the north. We also see several dwarf galaxies which show bridges with SPRC-188. The galaxy SDSS J033405.00+010541.0 to the west in the plane of the main body of SPRC-188 demonstrates a tidal feature which goes outwards. The overall shape is highly asymmetric and disturbed, possibly due to the recent formation of the PS (the ring also looks disturbed but does not have any fine structures connected to it) and interaction with several large neighbors (the irregular galaxy SDSS J033406.02+010615.0 to the north and the triplet of interacting galaxies to the east—all of them have concordant redshifts $z \sim 0.048$). We also note the prominent envelope around SPRC-188. Nevertheless, the overall profile of the host is exponential ($n = 1.0$) and red (probably due to dust, but the resolution is not enough to see a prominent dust lane). The profile of the PS is Gaussian ($n = 0.5$) and quite blue ($g - r = 0.22$). We suggest that the PS in SPRC-188 formed due to an encounter of the host with a less massive spiral galaxy ($L_{ps}/L_h = 0.22$). This event occurred quite long ago ($\gtrsim 2-3$ Gyr), so that we do not observe prominent tidal structures related to the polar ring.

SPRC-234: The central object in SPRC-234 is likely a highly inclined S0 galaxy ($n = 1.8$). The ordinary SDSS image of this galaxy does show a tilted structure with respect to the central body. However, the deep image displays it as a very faint two-armed spiral rather than a ring. Nevertheless, there is also a possibility that these spiral arms are tightly wound into a ring, similar to NGC 660. The average surface brightness along these arms is indeed very low ($\langle\mu_r\rangle \sim 26$ mag arcsec $^{-2}$ and the estimated arms-to-total ratio is unusually low: $f_r \sim 0.07$). This

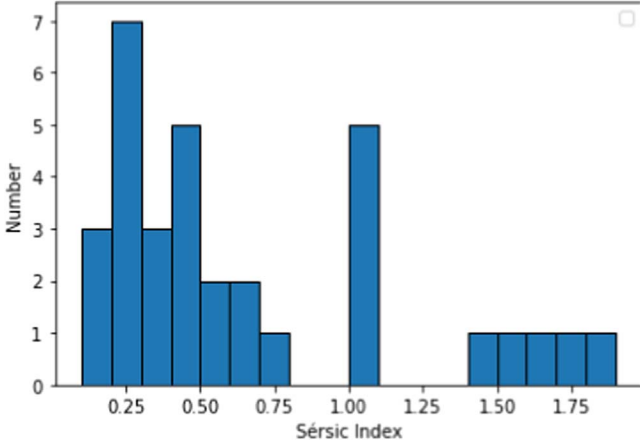


Figure 2. The distribution by the Sérsic index of PSs for the joined samples of PRGs from this study, Reshetnikov & Combes (2015) and Reshetnikov & Mosenkov (2019).

is inconsistent with what we observe as a rule in grand-design galaxies: Savchenko et al. (2020) find $\langle \mu_r \rangle \ll 25 \text{ mag arcsec}^{-2}$ and $f = 0.21 \pm 0.07$. The arms seem rather diffuse with no bright clumps of star formation. If we suppose that the red central object is not an S0 galaxy but a bar, its shape looks very unusual: the isophotes are pure elliptical in the inner region and become disk-like at the periphery, whereas bars in galaxies usually look boxy, but exceptions are also found (see e.g., Smirnov et al. 2021 and references therein). Furthermore, galaxy bars usually demonstrate truncated profiles along the major axis and their Sérsic indices are $n = 0.8 \pm 0.2$ (Gadotti 2009). Therefore, we can make a conclusion that either this object is a PRG host or that we observe a random projection of a lenticular galaxy on an open spiral.

We can see several small galaxies in the vicinity of SPRC-234 but their redshifts are unknown and we do not see any signs of interaction with the host galaxy. We can conclude that the nature of this object is uncertain and special observations are required.

SPRC-238: This galaxy shows multiple signatures of interaction with its neighbors which distorted its shape, such as an arc above the galaxy plane in the northwest direction. Perhaps, the other side of this PS is covered by the galaxy disk, so that we cannot observe it. The deep image demonstrates that there is a pronounced straight tidal tail to the east of the galaxy with a northeast direction. The color of this tail is similar to that of the host galaxy. The most plausible scenario for generating the observed PS in SPRC-238 is tidal disruption of a gas-rich dwarf ($L_{\text{ps}}/L_{\text{h}} \lesssim 0.1$), the debris of which is either covered by the host galaxy body, or completely stretched by the tidal forces, so that we do not see any nucleus left (although we note a small clumpy structure right above the plane).

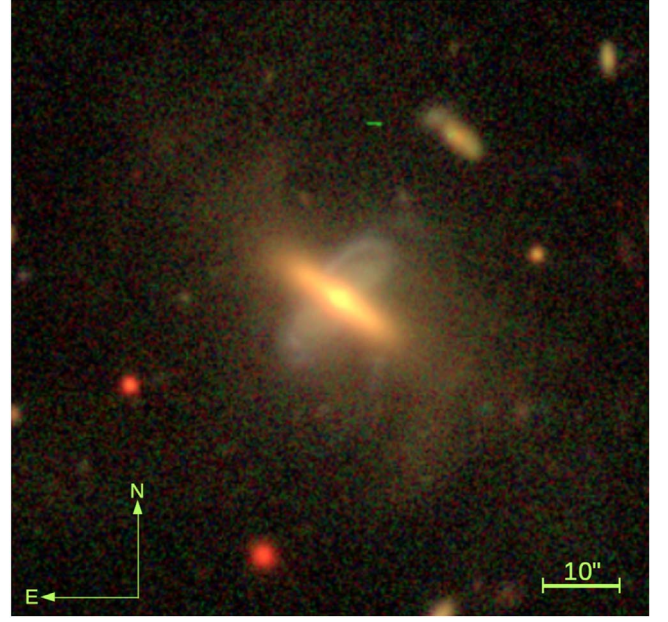


Figure 3. An RGB image for SPRC 28 from Subaru Hyper Suprime-Cam (Aihara et al. 2022). Note that the host galaxy has a faint disturbed envelope which consists of multiple tidal debris of past merger event(s).

SPRC-275: This galaxy is visually connected to its close twin, SDSS J205354.20-005814.3, although we cannot determine its redshift and confirm their real gravitational bound. Also, we do not see any faint structures in their vicinity. Although these two galaxies look similar, the main difference between them is the bluish color of the ring ($n = 0.2$) in SPRC-275, which points to a different origin of the observed structure. The central component in this galaxy is poorly resolved but its Sérsic index $n = 1.5$ is not typical of a bar. However, we can see a nucleus which may be, in fact, a tiny bulge embedded in a bar. The ring-to-host ratio $L_{\text{ps}}/L_{\text{h}} = 1.5$ is extremely large—only few galaxies out of the 50 PRGs in Reshetnikov & Combes (2015) have a ratio as large as 1.3. Also, the angle between the major axes of the host and the ring is the smallest in the sample, $\Psi = 19^\circ$ (see also Smirnova & Moiseev 2013). Therefore, we surmise that the blue ring in this galaxy lies in reality in the plane of the central structure which consists of a tiny bulge and a bar.

5. Discussion

In Section 4, we provided a detailed description of each galaxy in our sample. Exploring the properties of the host and the PS using photometric decomposition of the r -band Stripe 82 images allows us to draw some important conclusions.

The results for our sample are generally compatible with those obtained for a different sample of 50 PRGs by Reshetnikov & Combes (2015) and 31 PRGs by

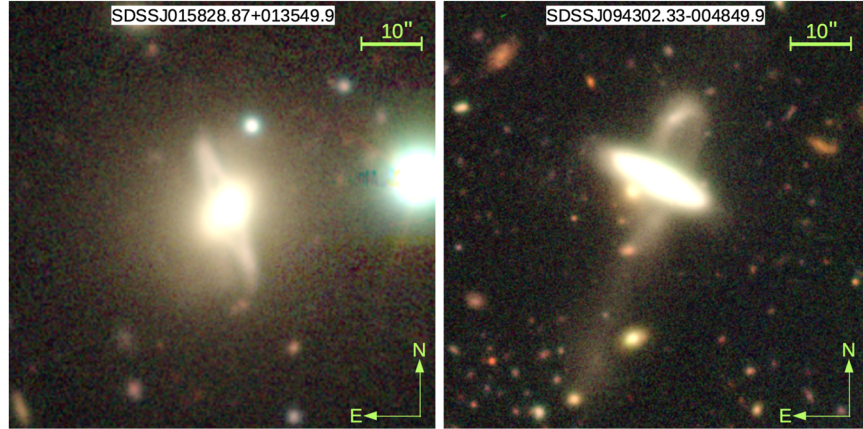


Figure 4. RGB images for two PRGs from Reshetnikov & Mosenkov (2019) based on Subaru Hyper Suprime-Cam observations. The left-hand image shows an envelope around the host and a warp of the polar ring. The right-hand image demonstrates the formation of a PS via a minor merger.

Reshetnikov & Mosenkov (2019) who used the same approach of modeling PRGs with two pure Sérsic components for a host and a ring.⁸ The ratio of the luminosity of the PS to the luminosity of the host varies in a wide range from 0.17 (SPRC-4) to 0.97 (SPRC-1), with an average value 0.50 ± 0.27 (0.38 ± 0.31 for the Reshetnikov & Combes 2015 sample), excluding SPRC-186 and 275. Our photometric decomposition of the latter two galaxies suggests that due to the outlying values of some of their parameters (e.g., the low projected angle between the major axes of the host and the PS and the very high host-to-ring ratio) these galaxies cannot be considered PRGs. The hosts in our sample are mostly lenticular galaxies with $n = 1.9 \pm 0.6$ ($n = 2.3 \pm 1.0$ in Reshetnikov & Combes 2015).

One of the main contributions of this paper is an analysis of the main parameters of the Sérsic model for the PSs. The Sérsic index is an important indicator of the morphology of a galaxy’s structure, which, for PSs, helps us conclude whether the luminous matter is distributed in the form of a ring ($n \lesssim 0.5\text{--}0.7$) or it has some other geometry. In Figure 2 we show the distribution by the Sérsic index of the polar components for the galaxies from our sample and those from Reshetnikov & Combes (2015) and Reshetnikov & Mosenkov (2019). As one can see, there are two groupings of the PSs: true polar rings with $n \lesssim 0.5\text{--}0.7$ and PSs with $n \gtrsim 1$, which may be polar disks (SPRC 28, see Figure 3), polar spheroids (SPRC 1 and SPRC 185), and only forming PSs (SPRC 73). Indeed, a photometrically distinctive polar “ring” can appear as a kinematically cold component, a disk, as shown by Iodice et al. (2002) for NGC 4650A. SPRC 185, as discussed in

⁸ Note that not all galaxies from the mentioned studies have estimates of the parameters for the host and PSs, as in some cases the host is too small to be fitted (only total magnitude is provided) or the polar ring is too faint to be modeled. In total, we collected the Sérsic parameters for 70 hosts and 40 PSs.

Section 4, has a red faint envelope which is significantly tilted with respect to the S0 host galaxy.

Although we know some PRGs in which the host and the ring have similar masses (for example, SPRC-3 and SPRC-35), usually the luminosity of the ring is 2–3 mag fainter than that of the host galaxy (see e.g., Finkelman et al. 2012; Reshetnikov & Combes 2015). However, our sample comprises rather bright polar rings as compared to their hosts: polar rings are mostly 0.5–1 mag fainter. Therefore, as our results suffer from the obvious selection bias, we limit ourselves to consider only those mechanisms which seem appropriate to drive the evolution of the sample galaxies.

In Section 4, we quantitatively described some general properties of the well-visible tidal features around three PRGs in our sample. Despite the large extent of these structures (up to ~ 70 kpc for SPRC-73), they typically contain only about 5% of the total galaxy light. This is consistent with what is usually observed around early-type galaxies (van Dokkum 2005). The LSB structures in and around the sample galaxies, also noted by us in Section 4, can provide important clues to the formation of these galaxies. In the Introduction, we summarized the main scenarios to form PRGs. Below we briefly discuss these mechanisms in the context of our results.

Major merging. In our sample, six galaxies (SPRC-1, 69, 73, 76, 77 and 185) show some evidence for this scenario. SPRC-1 resides in a very conducive environment for galaxy-galaxy interactions and mergers, in a compact group (Hickson 1997). Obviously, this galaxy has undergone one or several mergers. As we have shown in Section 4, one of the most remarkable results, which we obtained in our modeling, is that its polar dust ring is aligned with the polar stellar halo. We argue in favor of the scenario in which this PRG formed due to a major merger when one of the merging components was a gas- and dust-rich galaxy, whereas the second progenitor was a usual early-type galaxy. SPRC-73 and 76 are in process of the

formation of their PSs, and we can see a nucleus of the progenitor in this major merger. However, the question of whether these structures will be stable and not dissolve with time, creating an elliptical galaxy, remains open. In the case of SPRC-69, which has settled into an equilibrium, the polar ring might have formed due to a major merger, as the mass of the progenitor for the polar ring (possibly polar disk?) is considerable. An alternative scenario for this galaxy may be gas accretion.

Tidal accretion. This mechanism is the most plausible explanation for SPRC-74 and 238. These galaxies show very faint bridges of the material falling from the donor onto the PRG, similar to what is observed in the pair NGC 3808 (Ordenes-Briceño et al. 2016). This mechanism finds good observational support in the literature (see e.g., Reshetnikov et al. 2006; Moiseev 2008; Freitas-Lemes et al. 2012) and, thus, may explain some other observed PRGs in our sample (SPRC-4 and 69) where the polar rings are in a quasi-stable state, but no apparent accretion is seen in our deep images.

Cold accretion. In this scenario, PRGs form through the accretion of external cold gas from cosmic web filaments (see e.g., Brosch et al. 2007; Stanonik et al. 2009; Spavone et al. 2010). Gas infall along a filament may have a narrow angular momentum distribution and will settle into a ring structure (Brook et al. 2008). In principle, this mechanism can explain the formation of SPRC-4, 69 and 234 (if the latter galaxy is a true PRG). However, only deep photometric data are not sufficient to examine this scenario.

Disruption of a satellite. This scenario can be applicable to the explanation of the observed blue polar ring in SPRC-4 (taking into account the observed faint spiral trails around this galaxy) and the disk PS in SPRC-188. Also, one or several minor merger events can produce a halo around a galaxy (see e.g., Cooper et al. 2010). We propose that tidal disruption of accreted dwarf galaxies coupled with the misalignment of the triaxial (oblate) dark matter halo (van den Bosch et al. 2002; Chen et al. 2003; Sharma & Steinmetz 2005; Sharma et al. 2012) and its inner stellar disk might lead to the formation of a tilted stellar halo in this galaxy (see the discussion in Mosenkov et al. 2020 and references therein).

6. Summary

We have analyzed deep observations for 13 candidates of PRGs by exploiting deep images from SDSS Stripe 82 and other deep surveys. We summarize our results as follows:

1. For the selected galaxies, we enhanced the Stripe 82 data by stacking the three *gri* bands together. This allowed us to reach the depth $\mu_r \approx 30 \text{ mag arcsec}^{-2}$.
2. All galaxies under study, except SPRC-69, 186 and 275, demonstrate LSB structures in or around them: tidal features in a group (SPRC-1), tidal tails and streams (SPRC-4, 73, 74, 76, 185 and 238), arcs (SPRC-74 and

238), faint envelopes (SPRC-28, 77 and 185), extremely faint spiral arms or a (un)closed ring (SPRC-234). We suspect that LSB structures are probably nearly ubiquitous in these rare objects.

3. For SPRC-73, 76 and 188 we can directly observe the formation of the polar ring due to major or minor merging (see also Figure 4, right plot). In SPRC-73 and 76 we observe possible debris of the victim galaxy. We provide a qualitative description (see Section 4) and a quantitative analysis for three galaxies with distinctive tidal tails—SPRC-73, 76 and 238 (see Table 2).
4. In some cases (e.g., SPRC-69 and SDSSJ 015828.87 +013549.9 in Figure 4, left plot), there are no visible tidal features even in ultra-deep images, but the faint haloes and disrupted envelopes (see also Figure 3) suggest that the merger occurred several Gyr ago.
5. SPRC-74 demonstrates very faint signs of tidal accretion (see Figure A2). This is an additional proof of the importance of this mechanism in an effort to explain the formation of PRGs.
6. We carried out detailed photometric decomposition for all sample galaxies in the *r* passband to simultaneously fit the host and the PS. The advantage of this study is that we extract from the literature and study the structural parameters for both the polar rings and the hosts (see Table 3). This helps us estimate not only the morphology of the host, but also the morphology of the ring; 10 out of 40 galaxies from this study, Reshetnikov & Combes (2015) and Reshetnikov & Mosenkov (2019), harbor PSs with a Sérsic index $n \geq 1$ (see Figure 2). These PSs can be either spheroids or disks. Some of these structures are still forming: in many of them we can discern a disrupted core of the merging galaxy.

In our follow-up study, we are about to expand the sample of PRGs for which deep observations have been obtained. With upcoming large area sky surveys such as the Vera C. Rubin Observatory (formerly the Large Synoptic Survey Telescope, Ivezić et al. 2019), astronomy will soon be faced with a tremendous wealth of deep observations, which should help to reveal more LSB features around PRGs and test the existing formation mechanisms of these unique objects.

Acknowledgments

Aleksandr Mosenkov and Vladimir Reshetnikov acknowledge financial support from the Russian Science Foundation (Grant No. 22-22-00483) for developing an algorithm of enhancing deep optical imaging using modern sky surveys.

This research has made use of the NASA/IPAC Infrared Science Archive (IRSA; <http://irsa.ipac.caltech.edu/frontpage/>), and the NASA/IPAC Extragalactic Database (NED; <https://ned.ipac.caltech.edu/>), both of which are operated by the Jet Propulsion Laboratory, California Institute of Technology, under

contract with the National Aeronautics and Space Administration. This research has made use of the HyperLEDA database (<http://leda.univ-lyon1.fr/>; Makarov et al. 2014). This work is based in part on observations made with the Spitzer Space Telescope, which is operated by the Jet Propulsion Laboratory, California Institute of Technology under a contract with NASA.

Funding for the Sloan Digital Sky Survey IV has been provided by the Alfred P. Sloan Foundation, the U.S. Department of Energy Office of Science, and the Participating Institutions. SDSS-IV acknowledges support and resources from the Center for High-Performance Computing at the University of Utah. The SDSS website is www.sdss.org.

SDSS-IV is managed by the Astrophysical Research Consortium for the Participating Institutions of the SDSS Collaboration including the Brazilian Participation Group, the Carnegie Institution for Science, Carnegie Mellon University, the Chilean Participation Group, the French Participation Group, Harvard-Smithsonian Center for Astrophysics, Instituto de Astrofísica de Canarias, The Johns Hopkins University, Kavli Institute for the Physics and Mathematics of the Universe (IPMU)/University of Tokyo, the Korean Participation Group, Lawrence Berkeley National Laboratory, Leibniz Institut für Astrophysik Potsdam (AIP), Max-Planck-Institut für Astronomie (MPIA Heidelberg), Max-Planck-Institut für Astrophysik (MPA Garching), Max-Planck-Institut für Extraterrestrische Physik (MPE), National Astronomical Observatories of China, New Mexico State University, New York University, University of Notre Dame, Observatório Nacional/MCTI, The Ohio State University, Pennsylvania State University, Shanghai Astronomical Observatory, United Kingdom Participation Group, Universidad Nacional Autónoma de México, University of Arizona, University of Colorado Boulder, University of Oxford, University of Portsmouth, University of Utah, University of Virginia, University of Washington, University of Wisconsin, Vanderbilt University, and Yale University.

The Legacy Surveys consist of three individual and complementary projects: the Dark Energy Camera Legacy Survey (DECaLS; NOAO Proposal ID # 2014B-0404; PIs: David Schlegel and Arjun Dey), the Beijing-Arizona Sky Survey (BASS; NOAO Proposal ID # 2015A-0801; PIs: Zhou Xu and Xiaohui Fan), and the Mayall z-band Legacy Survey (MzLS; NOAO Proposal ID # 2016A-0453; PI: Arjun Dey). DECaLS, BASS and MzLS together include data obtained, respectively, at the Blanco telescope, Cerro Tololo Inter-American Observatory, National Optical Astronomy Observatory (NOAO); the Bok telescope, Steward Observatory, University of Arizona; and the Mayall telescope, Kitt Peak National Observatory, NOAO. The Legacy Surveys project is honored to be permitted to conduct astronomical research on Iolkam Du'ag (Kitt Peak), a mountain with particular significance to the Tohono O'odham Nation.

NOAO is operated by the Association of Universities for Research in Astronomy (AURA) under a cooperative agreement with the National Science Foundation.

This project used data obtained with the Dark Energy Camera (DECam), which was constructed by the Dark Energy Survey (DES) collaboration. Funding for the DES Projects has been provided by the U.S. Department of Energy, the U.S. National Science Foundation, the Ministry of Science and Education of Spain, the Science and Technology Facilities Council of the United Kingdom, the Higher Education Funding Council for England, the National Center for Supercomputing Applications at the University of Illinois at Urbana-Champaign, the Kavli Institute of Cosmological Physics at the University of Chicago, Center for Cosmology and Astro-Particle Physics at the Ohio State University, the Mitchell Institute for Fundamental Physics and Astronomy at Texas A&M University, Financiadora de Estudos e Projetos, Fundação Carlos Chagas Filho de Amparo, Financiadora de Estudos e Projetos, Fundação Carlos Chagas Filho de Amparo a Pesquisa do Estado do Rio de Janeiro, Conselho Nacional de Desenvolvimento Científico e Tecnológico and the Ministerio da Ciencia, Tecnologia e Inovacao, the Deutsche Forschungsgemeinschaft and the Collaborating Institutions in the Dark Energy Survey. The Collaborating Institutions are Argonne National Laboratory, the University of California at Santa Cruz, the University of Cambridge, Centro de Investigaciones Energeticas, Medioambientales y Tecnológicas-Madrid, the University of Chicago, University College London, the DES-Brazil Consortium, the University of Edinburgh, the Eidgenössische Technische Hochschule (ETH) Zurich, Fermi National Accelerator Laboratory, the University of Illinois at Urbana-Champaign, the Institut de Ciències de l'Espai (IEEC/CSIC), the Institut de Física d'Altes Energies, Lawrence Berkeley National Laboratory, the Ludwig-Maximilians Universität München and the associated Excellence Cluster Universe, the University of Michigan, the National Optical Astronomy Observatory, the University of Nottingham, the Ohio State University, the University of Pennsylvania, the University of Portsmouth, SLAC National Accelerator Laboratory, Stanford University, the University of Sussex, and Texas A&M University.

BASS is a key project of the Telescope Access Program (TAP), which has been funded by the National Astronomical Observatories of China, the Chinese Academy of Sciences (the Strategic Priority Research Program “The Emergence of Cosmological Structures” Grant No. XDB09000000), and the Special Fund for Astronomy from the Ministry of Finance. The BASS is also supported by the External Cooperation Program of Chinese Academy of Sciences (Grant No. 114A11KYSB20160057), and Chinese National Natural Science Foundation (Grant No. 11433005).

The Legacy Survey team makes use of data products from the Near-Earth Object Wide-field Infrared Survey Explorer (NEOWISE), which is a project of the Jet Propulsion

Laboratory/California Institute of Technology. NEOWISE is funded by the National Aeronautics and Space Administration.

The Legacy Surveys imaging of the DESI footprint is supported by the Director, Office of Science, Office of High Energy Physics of the U.S. Department of Energy under Contract No. DE-AC02-05CH1123, by the National Energy Research Scientific Computing Center, a DOE Office of Science User Facility under the same contract; and by the U.S. National Science Foundation, Division of Astronomical Sciences under Contract No. AST-0950945 to NOAO.

The Hyper Suprime-Cam (HSC) collaboration includes the astronomical communities of Japan and Taiwan, and Princeton University. The HSC instrumentation and software were developed by the National Astronomical Observatory of Japan (NAOJ), the Kavli Institute for the Physics and Mathematics of the Universe (Kavli IPMU), the University of Tokyo, the High Energy Accelerator Research Organization (KEK), the Academia Sinica Institute for Astronomy and Astrophysics in Taiwan (ASIAA), and Princeton University. Funding was contributed by the FIRST program from the Japanese Cabinet Office, the Ministry of Education, Culture, Sports, Science and Technology (MEXT), the Japan Society for the Promotion of Science (JSPS), Japan Science and Technology Agency (JST), the

Toray Science Foundation, NAOJ, Kavli IPMU, KEK, ASIAA, and Princeton University.

This paper makes use of software developed for Vera C. Rubin Observatory. We thank the Rubin Observatory for making their code available as free software at <http://pipelines.lsst.io/>.

This paper is based on data collected at the Subaru Telescope and retrieved from the HSC data archive system, which is operated by the Subaru Telescope and Astronomy Data Center (ADC) at NAOJ. Data analysis was in part carried out with the cooperation of Center for Computational Astrophysics (CfCA), NAOJ. We are honored and grateful for the opportunity of observing the universe from Maunakea, which has the cultural, historical and natural significance in Hawaii.

Appendix

Below, we provide supplementary images and decomposition results of the sample galaxies (Figures A1–A4).

Supplementary Images

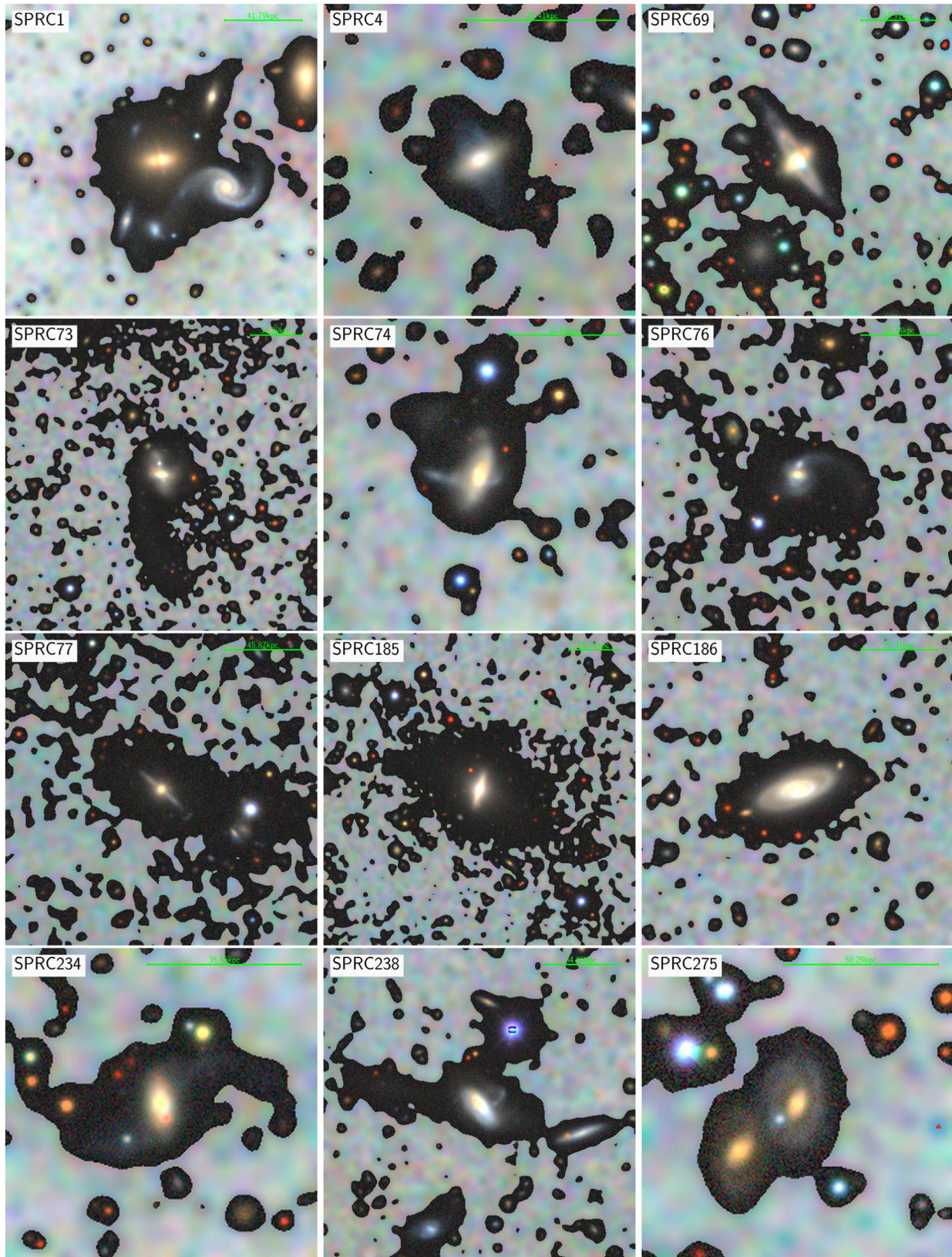


Figure A1. Enhanced DESI Legacy images for the PRG sample from this study. The darkish shadows correspond to surface brightnesses brighter than $27 \text{ mag arcsec}^{-2}$ in the r band. North is up and east is to the left. The scale bar depicts $30''$.

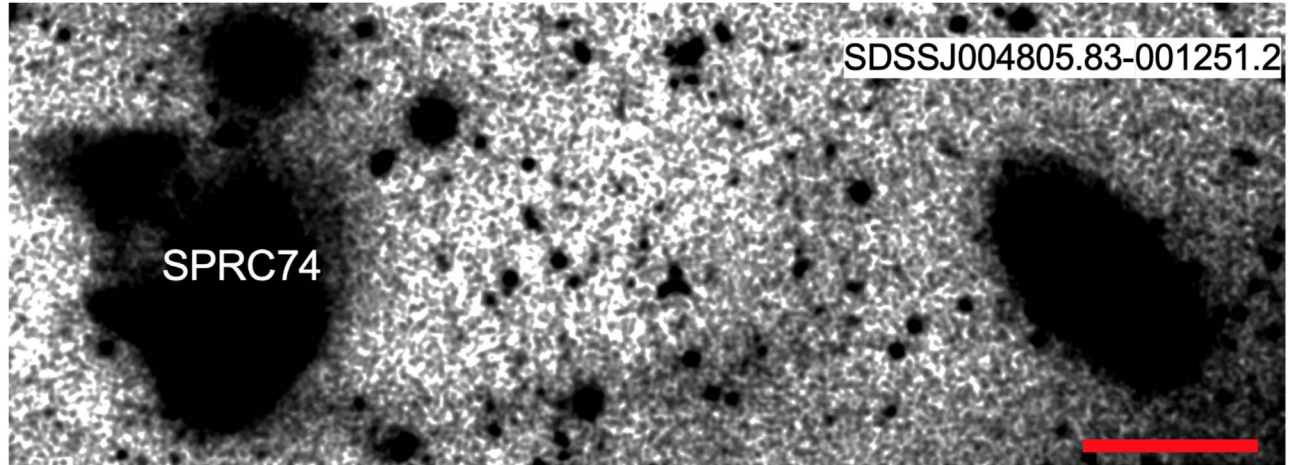


Figure A2. An RGB image of SPRC-74 from Subaru Hyper Suprime-Cam. North is up and east is to the left. The length of the bar in the bottom-right corner is 20".

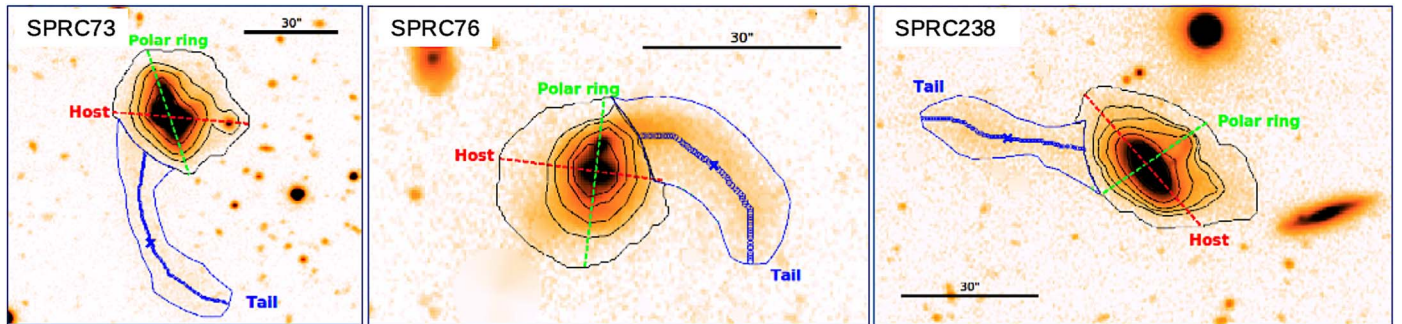


Figure A3. Description of the tidal tails in SPRC-73, SPRC-76 and SPRC-238. The dashed lines depict the axes of the structures: red—for the host, green—for the polar ring. The blue little circles show the centerline of the tail in each image. North is up and east is to the left.

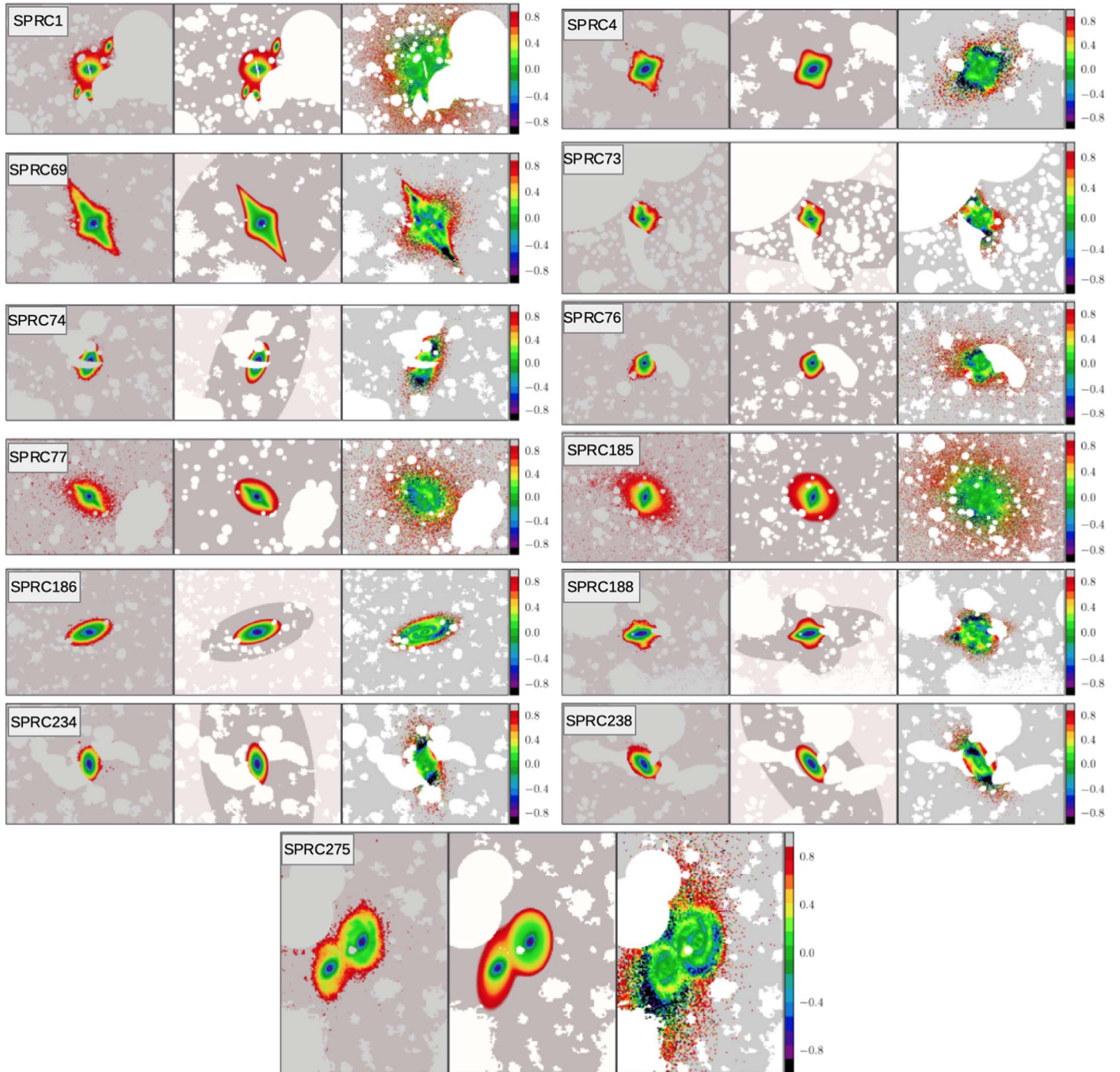


Figure A4. Results of our photometric decomposition for all sample galaxies in the r band: the observation (left), the model (middle) and the residual image (right), which indicates the relative deviation between the fit and the image.

ORCID iDs

Aleksandr V. Mosenkov  <https://orcid.org/0000-0001-6079-7355>

Zacory Shakespear  <https://orcid.org/0000-0002-1286-061X>

References

- Aguado, D. S., Ahumada, R., Almeida, A., et al. 2019, *ApJS*, **240**, 23
- Aihara, H., AIsayyad, Y., Ando, M., et al. 2022, *PASJ*, **74**, 247
- Bekki, K. 1997, *ApJL*, **490**, L37
- Bekki, K. 1998, *ApJ*, **499**, 635
- Bertin, E., & Armouts, S. 1996, *A&S*, **117**, 393
- Boucaud, A., Bocchio, M., Abergel, A., et al. 2016, *A&A*, **596**, A63
- Bournaud, F., & Combes, F. 2003, *A&A*, **401**, 817
- Brook, C. B., Governato, F., Quinn, T., et al. 2008, *ApJ*, **689**, 678
- Brosch, N., Kniazev, A. Y., Buckley, D. A. H., et al. 2007, *MNRAS*, **382**, 1809
- Burbidge, E. M., & Burbidge, G. R. 1959, *ApJ*, **130**, 20
- Chen, D. N., Jing, Y. P., & Yoshikaw, K. 2003, *ApJ*, **597**, 35
- Chilingarian, I. V., Melchior, A.-L., & Zolotukhin, I. Y. 2010, *MNRAS*, **405**, 1409
- Combes, F., Iodice, E., & Corsini, E. M. (ed.) 2014, in ASP Conf. Ser. 486, Multi-Spin Galaxies, Narrow Polar Rings versus Wide Polar Ring/Disk Galaxies (San Francisco, CA: ASP), 207
- Combes, F., Rampazzo, R., Bonfanti, P. P., Prugniel, P., & Sulentic, J. W. 1995, *A&A*, **297**, 37
- Cooper, A. P., Cole, S., Frenk, C. S., et al. 2010, *MNRAS*, **406**, 744
- Cooper, A. P., D'Souza, R., Kauffmann, G., et al. 2013, *MNRAS*, **434**, 3348
- Cooper, A. P., Parry, O. H., Lowing, B., Cole, S., & Frenk, C. 2015, *MNRAS*, **454**, 3185
- Dey, A., Schlegel, D. J., Lang, D., et al. 2019, *AJ*, **157**, 168
- Dobbs, C., & Baba, J. 2014, *PASA*, **31**, e035
- Duc, P.-A., Cuillandre, J.-C., Karabal, E., et al. 2015, *MNRAS*, **446**, 120
- Egorov, O. V., & Moiseev, A. V. 2019, *MNRAS*, **486**, 4186
- Erwin, P. 2015, *ApJ*, **799**, 226
- Finkelmann, I., Funes, J. G., & Brosch, N. 2012, *MNRAS*, **422**, 2386
- Finkelmann, I., Graur, O., & Brosch, N. 2010, *MNRAS*, **412**, 208
- Fliri, J., & Trujillo, I. 2016, *MNRAS*, **456**, 1359
- Font, A. S., McCarthy, I. G., Crain, R. A., et al. 2011, *MNRAS*, **416**, 2802
- Freitas-Lemes, P., Rodrigues, I., Faúndez-Abans, M., Dors, O. L., & Fernandes, I. F. 2012, *MNRAS*, **427**, 2772
- Fukugita, M., Ichikawa, T., Gunn, J. E., et al. 1996, *AJ*, **111**, 1748
- Gadotti, D. A. 2009, *MNRAS*, **393**, 1531
- Gorbatskii, V. G., & Korovyakovskii, Y. P. 1979, *SvAL*, **5**, 6
- Hibbard, J. E., & Mihos, J. C. 1995, *AJ*, **110**, 140
- Hickson, P. 1997, *ARA&A*, **35**, 357
- Infante-Sainz, R., Trujillo, I., & Román, J. 2020, *MNRAS*, **491**, 5317
- Iodice, E. 2014, in ASP Conf. Ser. 486, Multi-Spin Galaxies, Narrow Polar Rings versus Wide Polar Ring/Disk Galaxies, ed. E. Iodice & E. M. Corsini (San Francisco, CA: ASP), 39
- Iodice, E., Arnaboldi, M., De Lucia, G., et al. 2002, *AJ*, **123**, 195
- Iodice, E., Arnaboldi, M., Sparke, L. S., & Freeman, K. C. 2002, *A&A*, **391**, 117
- Jiang, L., Fan, X., Annis, J., et al. 2008, *AJ*, **135**, 1057
- Jiang, L., Fan, X., Bian, F., et al. 2014, *ApJS*, **213**, 12
- Johnston, K. V., Sackett, P. D., & Bullock, J. 2001, *ApJ*, **557**, 137
- Ivezić, Ž., Kahn, S. M., Tyson, J. A., et al. 2019, *ApJ*, **873**, 111
- Khoperskov, S. A., Moiseev, A. V., Khoperskov, A. V., & Saburova, A. S. 2014, *MNRAS*, **441**, 2650
- Knapp, G. R., Gallagher, J. S., Faber, S. M., & Balick, B. 1977, *AJ*, **82**, 106
- Maccio, A. V., Moore, B., & Stadel, J. 2006, *ApJL*, **636**, L25
- Makarov, D., Prugniel, P., Terekhova, N., Courtois, H., & Vauglin, I. 2014, *A&A*, **570**, A13
- Mancillas, B., Duc, P.-A., Combes, F., et al. 2019, *A&A*, **632**, A122
- McCarthy, I. G., Font, A. S., Crain, R. A., et al. 2012, *MNRAS*, **420**, 2245
- Miskolczi, A., Bomans, D. J., & Dettmar, R.-J. 2011, *A&A*, **536**, A66
- Moiseev, A., Egorov, O., & Smirnova, K. 2014, ASPC, **486**, 71
- Moiseev, A. V. 2008, *AstBu*, **63**, 201
- Moiseev, A. V., Smirnova, K. I., Smirnova, A. A., & Reshetnikov, V. P. 2011, *MNRAS*, **418**, 244
- Morales, G., Martínez-Delgado, D., Grebel, E. K., et al. 2018, *A&A*, **614**, A143
- Mosenkov, A., Rich, R. M., Koch, A., et al. 2020, *MNRAS*, **494**, 1751
- Mosenkov, A. V., Smirnov, A. A., Sil'chenko, O. K., et al. 2020, *MNRAS*, **497**, 2039
- Mould, J., Balick, B., Bothun, G., & Aaronson, M. 1982, *ApJL*, **260**, L37
- Ordenes-Briceño, Y., Georgiev, I. Y., Puzia, Th. H., Goudfrooij, P., & Arnaboldi, M. 2016, *A&A*, **585**, A156
- Rampazzo, R., Omizzolo, A., Usleghi, M., et al. 2020, *A&A*, **640**, A38
- Ren, J., Zheng, X. Z., Valls-Gabaud, D., et al. 2020, *MNRAS*, **499**, 3399
- Reshetnikov, V., Bournaud, F., Combes, F., et al. 2005, *A&A*, **431**, 503
- Reshetnikov, V., Bournaud, F., Combes, F., Faúndez-Abans, M., & de Oliveira-Abans, M. 2006, *A&A*, **446**, 447
- Reshetnikov, V., & Combes, F. 2015, *MNRAS*, **447**, 2287
- Reshetnikov, V., & Sotnikova, N. 1997, *A&A*, **325**, 933
- Reshetnikov, V. P., & Combes, F. 1994, *A&A*, **291**, 57
- Reshetnikov, V. P., Faúndez-Abans, M., & de Oliveira-Abans, M. 2011, *AstL*, **37**, 171
- Reshetnikov, V. P., Hagen-Thorn, V. A., & Yakovleva, V. A. 1996, *A&A*, **314**, 729
- Reshetnikov, V. P., & Mosenkov, A. V. 2019, *MNRAS*, **483**, 1470
- Rich, R. M., Mosenkov, A., Lee-Saunders, H., et al. 2019, *MNRAS*, **490**, 1539
- Savchenko, S., Marchuk, A., Mosenkov, A., & Grishunin, K. 2020, *MNRAS*, **493**, 390
- Schlaflly, E. F., & Finkbeiner, D. P. 2011, *ApJ*, **737**, 103
- Schlegel, D. J., Finkbeiner, D. P., & Davis, M. 1998, *ApJ*, **500**, 525
- Schweizer, F., Whitmore, B. C., & Rubin, V. C. 1983, *AJ*, **88**, 909
- Sérsic, J. L. 1967a, Boletín de la Asociación Argentina de Astronomía La Plata Argentina, **6**, 41
- Sérsic, J. L. 1967b, Zeitschrift für Astrophysik, **67**, 306
- Sérsic, J. L. 1968, Atlas de Galaxias Australes. Observatorio Astronomico, Cordoba, Argentina
- Shane, W. W. 1980, *A&A*, **82**, 314
- Sharma, S., & Steinmetz, M. 2005, *ApJ*, **628**, 21
- Sharma, S., Steinmetz, M., & Bland-Hawthorn, J. 2012, *ApJ*, **750**, 107
- Smirnov, A. A., Tikhonenko, I., & Sotnikova, N. Y. 2021, *MNRAS*, **502**, 4689
- Smirnova, K. I., & Moiseev, A. V. 2013, *AstBu*, **68**, 371
- Sola, E., Duc, P.-A., Richards, F., et al. 2022, *A&A*, **662**, A124
- Spavone, M., Iodice, E., Arnaboldi, M., et al. 2010, *ApJ*, **714**, 1081
- Stanonik, K., Platen, E., Aragón-Calvo, M. A., et al. 2009, *ApJL*, **696**, L6
- Teeninga, P., Moschini, U., Trager, S. C., & Wilkinson, M. H. 2015, in Int. Symp. on Mathematical Morphology and Its Applications to Signal and Image Processing (Cham: Springer), 157
- Thakar, A. R., & Ryden, B. S. 1996, *ApJ*, **461**, 55
- Thakar, A. R., & Ryden, B. S. 1998, *ApJ*, **506**, 93
- Toomre, A. 1977, in Evolution of Galaxies and Stellar Populations, Proc. Conf. at Yale University, ed. B. M. Tinsley, B. Larson Richard, & D. C. Gehret (Yale University Observatory, New Haven, CN), 401
- van den Bosch, F. C., Abel, T., Croft, R. A. C., Hernquist, L., & White, S. D. M. 2002, *ApJ*, **576**, 21
- van Dokkum, P. G. 2005, *AJ*, **130**, 2647
- van Gorkom, J. H., Schechter, P. L., & Kristian, J. 1987, *ApJ*, **314**, 457
- Whitmore, B. C., Lucas, R. A., McElroy, D. B., et al. 1990, *AJ*, **100**, 1489
- Whitmore, B. C., McElroy, D. B., & Schweizer, F. 1987, *ApJ*, **314**, 439